"String-of-Beads" Flow of Liquids on Vertical Wires for Gas Absorption

Hirofumi Chinju, Kazunori Uchiyama, and Yasuhiko H. Mori
Dept. of Mechanical Engineering, Keio University, Yokohama 223-8522, Japan

A liquid steadily fed onto a thin wire vertically held in a gas stream may flow down the wire, taking the form of a "string of beads," which is a composite of teardrop-shaped beads regularly aligned on the wire and thin cylindrical films each coating the portion of the wire between two neighboring beads. The beads slide down at a constant speed, interacting with the films flowing down much more slowly, thereby inducing some mixing motion in the liquid phase. The string-of-beads flow exhibited by water or an aqueous monoethanolamine solution was observed, and the mass transfer of CO_2 from the surrounding CO_2/N_2 mixture into water flowing down single wires was studied both experimentally and analytically. The results indicate the potential of on-wire string-of-beads flow devices for innovating gas–liquid contact operations to be used in, for example, removing CO_2 from flue gases exhausted at fossil-fuel-fired power plants.

Introduction

When a liquid is continuously supplied onto a vertically oriented wire (or a thread) well wettable with the liquid, a particular flow pattern may appear that we here call a "string of liquid beads." This flow pattern is apparently characterized by regularly aligned teardrop-shaped beads that are sliding down the wire, keeping their intervals uniform and constant. The portions of the wire surface not covered by those beads at each instant are covered by thin, cylindrical liquid-films that are flowing down at a much lower velocity. There is no dry area over the wire surface; any point on the wire surface is covered by beads and films alternately.

If a number of wires are hung in a stream of a gas or gas mixture so that a liquid flows down those wires in the form of strings of liquid beads, both a large gas–liquid interfacial area and a long contact time may be obtained simultaneously even with the limited fall distance of the liquid. Noting these features of the string-of-beads flow, Hattori et al. (1994) proposed to apply it to thermal-energy recovery from hot gases. Recently, Nozaki et al. (1998) reported on an experimental study of heat transfer to a liquid flowing down a vertical wire from a surrounding, countercurrent air flow.

Because of a significant difference in fall velocity between the beads and the films aligned on each wire, the string-of-beads flow may sustain considerable mixing in the liquid phase. Based on this idea, we can presume that the string-of-beads flow may be more suited for interphase mass-transfer operations, than for heat-transfer operations, in which the diffusional resistance in the liquid phase is generally rate controlling. This is the motivation of the studies compiled in this article: they are (1) observations of on-wire flow of water and an aqueous monoethanolamine solution, the liquids to be used as absorbents of carbon dioxide (CO_2); (2) a model analysis of gas absorption by a liquid in the string-of-beads flow; (3) experiments of CO_2 absorption by water in the string-of-beads flow; and (4) comparison of vertical-wire columns utilizing the string-of-beads flow with conventional gas–liquid contactors (wetted-wall and packed-bed columns) used for CO_2-into-water absorption. Those studies are described in order, leading to the conclusion that the vertical-wire columns have significant advantages over conventional contactors when the solute absorbed from the gas phase is desired to be highly concentrated in the liquid absorbent. These advantages indicate the utility of the vertical-wire columns in removing toxic species from industrial exhaust

Correspondence concerning this article should be addressed to Y. H. Mori.
Current addresses of: N. Chinju, Department of Quantum Engineering and Systems Science, University of Tokyo, 7-3-1 Hongo, Bunkyo-ku, Tokyo 113-8656, Japan; K. Uchiyama, Nippon Soken, Inc., 14 Iwaya, Shimohasumi-cho, Nishio-shi, Aichi-ken 445-0012, Japan.

gases or CO_2, a greenhouse effect gas, from the flue gases exhausted at fossil-fuel-fired power plants.

Liquid Flow on Wires: Experimental Observations

Pure water and a 50-wt % aqueous solution of MEA (monoethanolamine) were selected as model absorbents, and their flow behavior on vertical wires was first investigated. Pure water was used extensively, while the MEA solution was used only complementarily. In the experiments with water, glass wires 0.65–1.07 mm in diameter were used exclusively; this is because we found no wire material, other than glass, that was completely wet by water. The MEA solution was found to wet wires made from various materials, and hence both glass and stainless-steel wires were employed for use in the experiments with the solution.

Hattori et al. (1994) observed the flow of silicone oils fed onto vertical wires 0.3–0.5 mm in diameter and found several different flow patterns, depending on the viscosity of the oils and the flow rate on each wire. Despite large differencces in physical properties between the silicone oils and water, we found that the flow-pattern variation exhibited by water, depending on its flow rate, is qualitatively the same as that observed with the silicone oils. The present observations with water were limited to a flow-rate range in which the regular string-of-beads flow pattern, that is, pattern B defined in Hattori et al. (1994), prevails. The motivation of the present observations was a suspicion of the notion underlying the study of Hattori et al. (1994): that is, the notion that once the flow rate and the wire diameter, as well as the liquid substance and the thermodynamic condition, are prescribed, the flow behavior characterized by the size and the axial intervals of liquid beads is uniquely determined at locations sufficiently away from the nozzle through which the liquid is supplied onto the wire. This notion would keep us from considering the nozzle–wire assembly if we are exclusively concerned with the *developed* liquid flow on the wire. In the present study, we have experimentally found that even the developed flow behavior on a given wire at a prescribed flow rate is dependent on the configuration of the nozzle–wire assembly.

Apparatus and procedure

The configurations of the nozzle–wire assembly tested in this study are limited to the case of the vertically oriented, concentric arrangement illustrated in Figure 1. The inside diameter of a tubular nozzle, d_n, or the nozzle–wire clearance $(d_n - d_w)/2$, relative to the wire diameter, d_w, was one of the two operational parameters; the other parameter was the liquid flow rate, $\dot{V}_L$.

The experiments were performed in a laboratory temperature-controlled at 20 ± 1°C. Deionized and distilled water, or the MEA solution, was supplied to the nozzle from a reservoir pressurized by nitrogen gas. The flow rate of the liquid was controlled and measured by an electronic mass-flow controller set on the line from the reservoir to the nozzle. The string of beads on the wire was photographed so that we could measure, on high magnification pictures, the vertical and horizontal dimensions, d_{d1} and d_{d2}, of individual beads as well as the diameter d_f of cylindrical films and, on low magnification pictures, the axial intervals of the beads, l_d. Typical low-magnification pictures are exemplified in Figure 2. The frequency of bead passages at an arbitrary location on the wire was measured by a stroboscope, and the fall velocity of the beads, U_d, was calculated from l_d and the frequency thus measured.

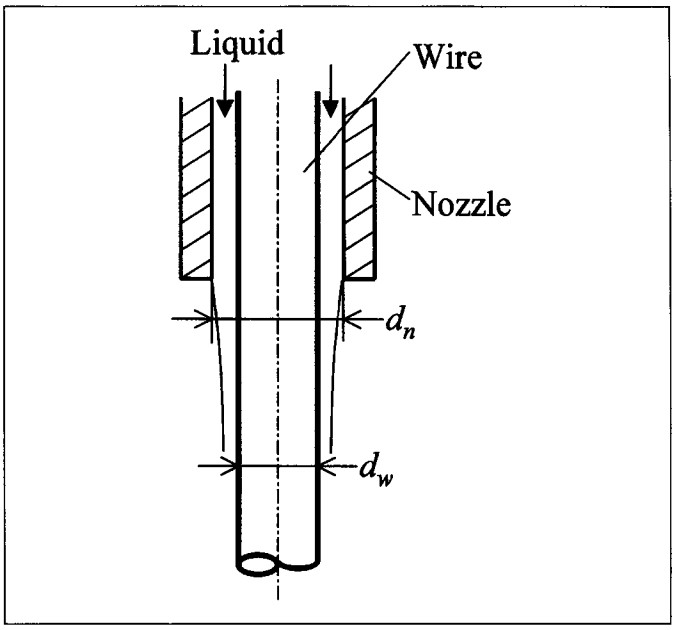

Figure 1. Concentric nozzle–wire assembly.

Throughout the experiments, we empirically found that the flow behavior is very sensitive to even a slight loss of concen-

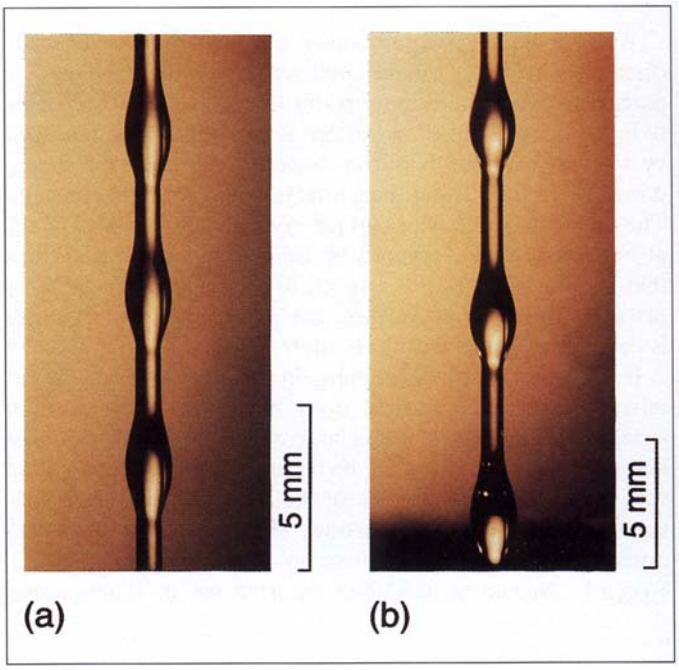

Figure 2. Typical pictures of string-of-beads flow.

(a) Water on a glass wire, $d_w = 0.85$ mm, $d_n = 0.90$ mm, $\dot{V}_L = 34.2$ mm^3/s; (b) MEA solution on a glass wire, $d_w = 0.72$ mm, $d_n = 0.90$ mm, $\dot{V}_L = 69.6$ mm^3/s.

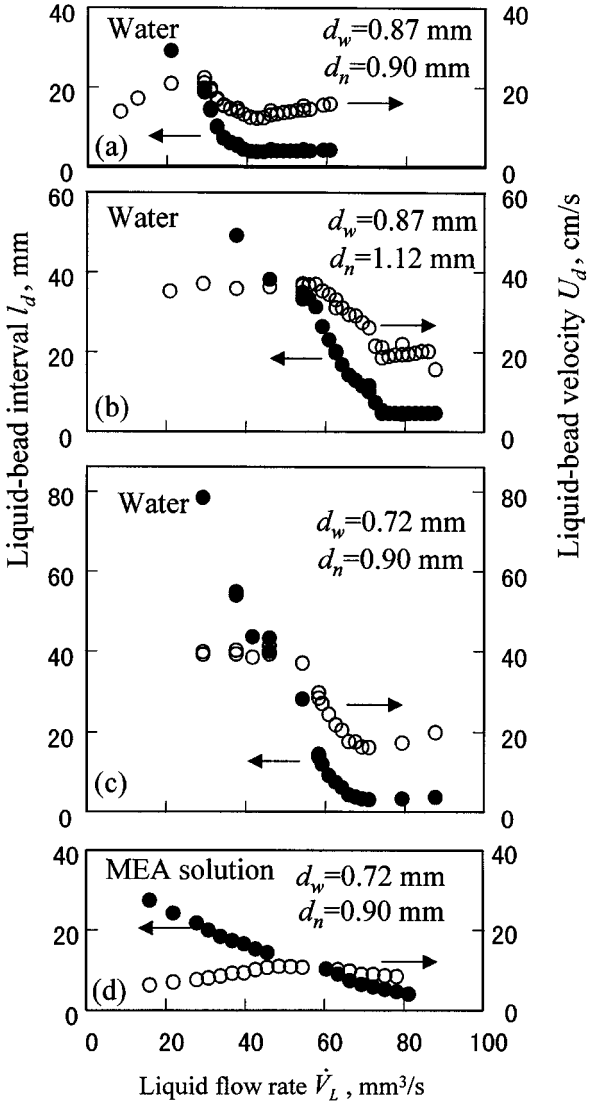

Figure 3. Variations in axial interval l_d and fall velocity U_d of beads with volume flow rate $\dot{V}_L$.

tricity in the nozzle–wire assembly. The bead interval l_d tends to shorten with an increasing eccentricity in the assembly. Thus, we carefully adjusted the nozzle–wire assembly before each experiment so that l_d was maximized.

Results and discussion

Figure 3 contains four diagrams, (a) to (d), each showing the variations in l_d and U_d depending on $\dot{V}_L$ for a particular $d_w - d_n$ combination. The first three of them, (a) to (c), are for pure water, while the fourth, (d), is for the MEA solution. Note that d_w is the same in the (a)–(b) pair, while d_n is the same in the (a)–(c) pair, and both d_w and d_n are the same in the (c)–(d) pair. We note particular patterns in the l_d–$\dot{V}_L$ and U_d–$\dot{V}_L$ relations, which are common to most of the d_w–d_n combinations we tested: l_d monotonically decreases with an increase in $\dot{V}_L$ up to a critical flow rate, $\dot{V}_{L,\mathrm{cr}}$, beyond which l_d levels off, while U_d first increases, though only gradually, with an increase in $\dot{V}_L$, until it peaks at a flow rate

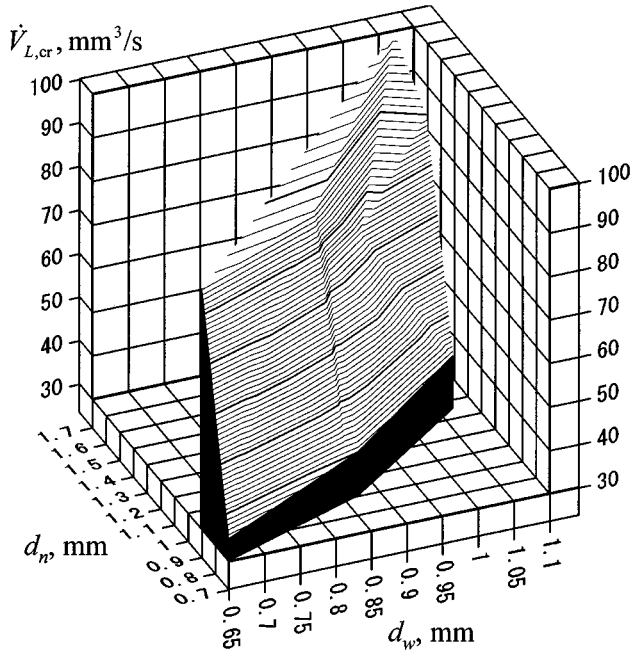

Figure 4. Comprehensive representation of critical flow rate $\dot{V}_{L,\mathrm{cr}}$ of water beyond which l_d levels off.

about two thirds of $\dot{V}_{L,\mathrm{cr}}$, then decreases rather sharply to a minimum at a flow rate equal to $\dot{V}_{L,\mathrm{cr}}$, beyond which U_d tends to increase again. The $\dot{V}_L$ value corresponding to the rightmost data points in each diagram is very close to the maximum flow rate for the stable string-of-beads flow pattern, $\dot{V}_{L,\max}$, beyond which the flow behavior becomes irregular. In general, an increase in the nozzle–wire clearance, $(d_n - d_w)/2$, causes increases in both $\dot{V}_{L,\mathrm{cr}}$ and $\dot{V}_{L,\max}$. The increase in $\dot{V}_{L,\mathrm{cr}}$, however, is sharper than that in $\dot{V}_{L,\max}$, thus resulting in the disappearance of the constant l_d region in l_d–$\dot{V}_L$ relations with relatively large clearances. The absence of such a constant l_d region in diagram (d) may be ascribable to a reduction in $\dot{V}_{L,\max}$, with an increase in the viscosity of the liquid, that is greater than that in $\dot{V}_{L,\mathrm{cr}}$. (Note that the 50 wt % MEA solution has a kinematic viscosity that is about five times that of pure water). The l_d–$\dot{V}_L$ relations observed in the experiments with pure water are summarized in Figure 4 to illustrate the variation in $\dot{V}_{L,\mathrm{cr}}$ depending on d_w and d_n.

Figure 5 shows the variations in bead/film dimensions observed in two particular experimental settings, one relevant to diagram (c) and the other to diagram (d) in Figure 3. The dimensions plotted here are the axial length d_{d1}, the maximum diameter d_{d2}, and the equivalent spherical diameter, d_d, defined as $(d_{d1}d_{d2}^2)^{1/3}$, of the beads and also the cylindrical-film diameter d_f. It is noted that the bead dimensions observed with pure water show minima at a flow rate equal to $\dot{V}_{L,\mathrm{cr}}$, which can be seen in diagram (c) in Figure 3. The bead dimensions for the MEA solution do not show any distinct minimum, consistent with the absence of $\dot{V}_{L,\mathrm{cr}}$ in diagram (d) in Figure 3. Combining Figures 3 and 5, it may be said that an increase in $\dot{V}_L$ up to $\dot{V}_{L,\mathrm{cr}}$ is borne by an increase in the number density of beads, while that beyond $\dot{V}_{L,\mathrm{cr}}$ is borne by increases in the size and fall velocity of individual beads. On the other hand, it should be noted that $\dot{V}_L$ cannot

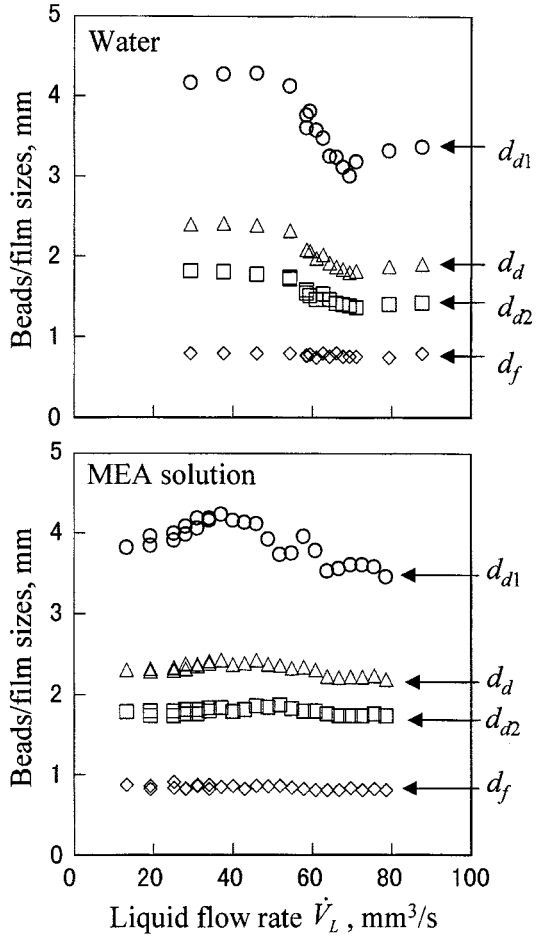

Figure 5. Variations in axial length d_{d1}, maximum diameter d_{d2}, and equivalent spherical diameter d_d of beads and of cylindrical-film diameter d_f with liquid flow rate: d_w = 0.72 mm; d_n = 0.90 mm.

be simply divided into two parts conveyed by the beads and by the films. This is because the beads and the films are not isolated elements; the liquid must continuously flow into and out of each bead or film. This presumption is supported by an interesting fact that the apparent bead-conveyed liquid flow rate given by $V_d U_d / l_d$ appreciably exceeds the corresponding total liquid flow rate, $\dot{V}_L$.

Model Analysis of Gas Absorption by Liquid in String-of-Beads Flow

Described below is a simple model that we can use to estimate the characteristics of a string-of-beads liquid flow as a means of absorbing a particular species from the surrounding gas mixture in the absence of any chemical reaction related to the species. This model bears a close resemblance to "model II" for the gas-to-liquid heat transfer described in Hattori et al. (1994). The primary difference between these two models is in the way we account for the component resistances to the mass/heat transfer. The heat-transfer model considers the convective resistances in the gas phase and liquid beads, neglecting the resistance in the cylindrical films. On the other hand, the present absorption (mass-transfer) model considers the resistances in the beads and the films, neglecting the resistance in the gas phase. This is because liquid mixtures generally have much lower mass diffusivities than gaseous mixtures. The specific assumptions used in the present model are:

1. The films and the beads on a wire are monosized cylinders (diameter d_f) and spheres (diameter d_d), respectively, both coaxial with the wire and aligned on the wire at uniform intervals.

2. The fall velocity of the beads, U_d, and the flow velocity in each film averaged over its cross section, U_f, are held constant, while falling on the wire.

3. Because $U_d \gg U_f$, each bead continuously engulfs the film ahead of itself and, at the same time, *spins* another film at its rear in such a way that the film initially has the same mixed-mean concentration of the transferred species as that in the bead.

4. The liquid-side concentration of the transferred species, c, at the gas–liquid interface (that is, the surfaces of the films and the beads) is held at c_s, the solubility corresponding to the partial pressure of the species in the surrounding gas flow.

5. The coefficient for the surface-to-bulk transfer of the species inside each bead, β_d, is given by the Kronig–Brink solution for the asymptotic mass transfer inside a fluid sphere with toroidal internal circulation.

6. A self-similar, radial c profile prevails throughout the films.

7. The axial diffusion of the transferred species in the films can be neglected.

8. The physical properties of the gas and the liquid are constant irrespective of the spatial variation in the concentration.

Because of the lack of hydrodynamic theory to describe the string-of-beads flow, we inevitably rely on experimental observations to evaluate some of the geometrical and dynamic parameters used in formulating the model: they are d_d, d_f, U_d, and τ, the time interval between successive passings of beads observed at a fixed location on the wire. The average film velocity U_f cannot be determined by simple observations; hence, it is approximated by an analytic solution for a fully developed annular-film flow on the wire [see appendix B in Hattori et al. (1994)] such that:

$$U_f = \frac{g d_w^2}{32 \nu_L}\left(1 - 3a^2 + 4\frac{a^4 \ln a}{a^2 - 1}\right), \tag{1}$$

where g is the acceleration due to gravity, ν_L is the kinematic viscosity of the liquid, and $a \equiv d_f / d_w$.

Concerning the validity of assumption 5, consult Hattori et al. (1994). This assumption enables us to evaluate β_d as

$$Sh_d \equiv \frac{\beta_d d_d}{D} = 17.66, \tag{2}$$

where D is the mass diffusivity of the transferred species in the liquid. Assumption 6 can be used to express the radial distribution of c over an arbitrary cross section of a film by a

quadratic function such that

$$\frac{c - c_w}{c_s - c_w} = \left(\frac{r - R_w}{R_f - R_w} \right)^2, \tag{3}$$

where c_w is c at $r = R_w$; r is the radial coordinate with its origin laid on the wire axis; R_w is the radius of the wire ($= d_w/2$); and R_f is the outer radius of the film ($= d_f/2$). Note that Eq. 3 satisfies the boundary condition prescribing no mass flux on the wire surface:

$$r = R_w: \quad \partial c/\partial r = 0. \tag{4}$$

Following a procedure analogous to the analysis of heat transfer in an annular film, which is described in appendix C in Hattori et al. (1994), we can derive from Eqs. 3 and 4 the following expression for β_f, the mass-transfer coefficient in the film:

$$Sh_f \equiv \frac{\beta_f (R_f - R_w)}{D} = 2\left[1 - \left(\frac{R_w}{R_f - R_w} \right)^2 G(a) \right]^{-1}, \tag{5}$$

where $G(a)$ is a function of a such that

$$G(a) = \frac{4}{4a^2 - 3a^4 - 1 + 4a^4 \ln a}\left[-\frac{1}{15} + \frac{49}{72}a^2 - \frac{2}{3}a^3 - \frac{1}{2}a^4 + \frac{38}{45}a^5 - \frac{7}{24}a^6 + \left(a^4 - \frac{4}{3}a^5 + \frac{1}{2}a^6 \right) \ln a \right]. \tag{6}$$

The equation for transferred-species conservation for a unit-length element of a film and that for each bead are written, respectively, as follows:

$$S_f \frac{dc_f}{dt} = \pi d_f \beta_f (c_s - c_f) \tag{7}$$

$$V_d \frac{dc_d}{dt} = A_d \beta_d (c_s - c_d) + S_f (U_d - U_f)(c_f - c_d), \tag{8}$$

where c_f and c_d are mixed-mean concentrations in the film and the bead, respectively; S_f, V_d, and A_d are the cross-sectional area of the film, the volume of the bead, and the surface area of the bead, respectively, which are defined as

$$S_f = \frac{\pi}{4}(d_f^2 - d_w^2)$$

$$V_d = \pi \left(\frac{d_d^3}{6} - \frac{d_d d_w^2}{4} \right)$$

$$A_d = \pi \left(d_d^2 - \frac{d_f^2}{2} \right).$$

Note that c_d is assumed to be a function of x at the front of the bead and that, in Eq. 8, c_f is the mixed-mean concentration in the film at the x-axial location where the bead front just arrives, where x denotes the vertical coordinate down from the nozzle tip through which the liquid is issuing. The initial condition to be coupled with Eqs. 7 and 8 may be a specification of the concentration c_{L0} in the liquid before issuing into the gas stream: that is,

$$t = 0: \quad x = 0, \quad c_f = c_d = c_{L0}. \tag{9}$$

Equations 7–9 can be solved for $c_f(x)$ and $c_d(x)$ by the iterative procedure described below.

First we assume $c_f(x)$ arbitrarily, which is designated $c_{f1}(x)$. Then, by substituting $c_{f1}(x)$ into Eq. 8 and integrating it numerically, we calculate the concentration $c_{d1}(x)$ that a bead will have while falling down the wire and thereby interacting with the film with concentration $c_{f1}(x)$. A film element *spun* at the rear end of the bead is exposed to the gas stream for a period τ_{fg} and then meets the front of a second bead. The concentration in the film at this instant, $c_{f2}(x)$, is obtained by integrating Eq. 7 over the period τ_{fg}, noting that the film element that meets the front of the second bead at a location x must have been *spun* at the location $x - U_f\tau_{fg}$ from the first bead, the front of which was located at $x - U_f\tau_{fg} + d_d$:

$$\frac{c_{f2}(x) - c_{d1}(x - U_f\tau_{fg} + d_d)}{c_s - c_{d1}(x - U_f\tau_{fg} + d_d)} = 1 - \exp\left(-\frac{\pi d_f \beta_f \tau_{fg}}{S_f} \right), \tag{10}$$

where τ_{fg} is related to τ as

$$\tau_{fg} = \frac{U_d\tau - d_d}{U_d - U_f}.$$

The concentration $c_{d2}(x)$ that the second bead will have is obtained by substituting $c_{f2}(x)$ given by Eq. 10 back into c_f in Eq. 8 and integrating it again. Such calculations for $c_{fi}(x)$ and $c_{di}(x)$ [$i = 1, 2, 3, \ldots$] should be continued, assuming the periodic passings of beads, until $c_{fi}(x)$ and $c_{di}(x)$ become invariable with a further increase in i. The asymptotic values of $c_{fi}(x)$ and $c_{di}(x)$ thus obtained are considered to be the solutions of Eqs. 7 and 8, that is, $c_f(x)$ and $c_d(x)$. Once $c_f(x)$ and $c_d(x)$ are determined, we can immediately calculate $c_L(x)$, the time-averaged mixed-mean concentration in the liquid at each axial location, as

$$c_L(x) = \frac{c_f(x) S_f U_f + c_d(x) V_d/\tau}{S_f U_f + V_d/\tau}. \tag{11}$$

Some predictions due to the model just described are shown later, in comparison with relevant experimental results.

Experiments of CO_2 Absorption by Water in String-of-Beads Flow

The present experiments were designed to study the absorption of CO_2 from a gas mixture in a steady flow by pure water flowing down a vertically oriented single wire. The gas mixture was a binary blend of 11-mol % CO_2 and 89-mol % N_2, which can simulate the flue gases exhausted at fossil-fuel-fired power plants.

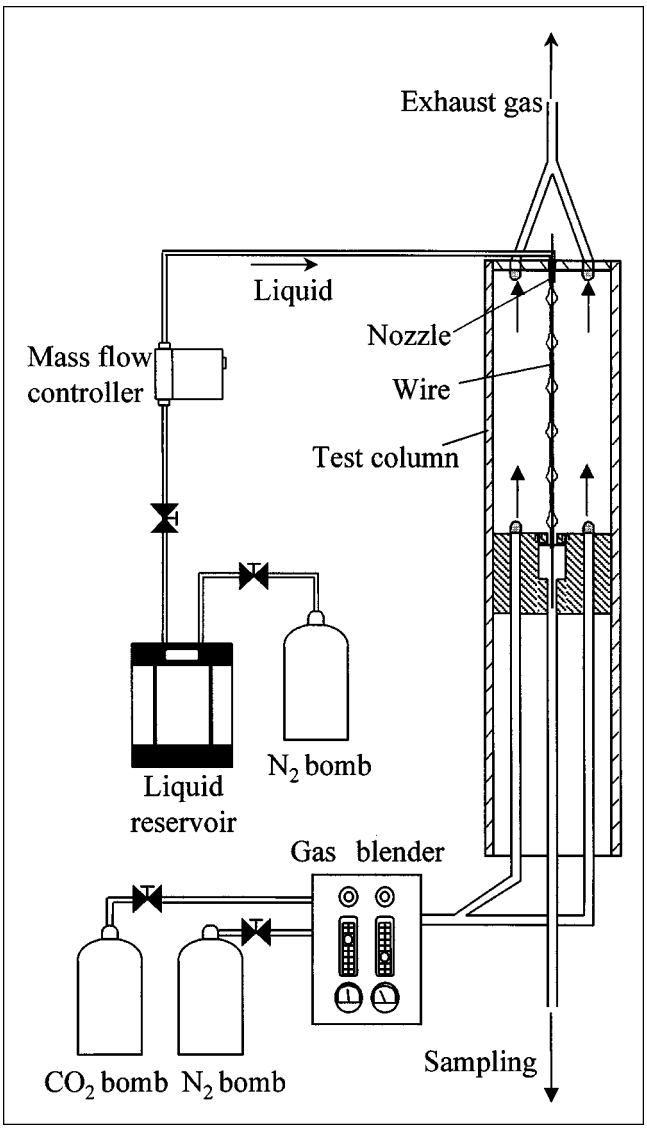

Figure 6. Experimental setup for measuring CO_2 concentration in water having flowed down a wire countercurrently with N_2/CO_2 gas mixture.

Apparatus and procedure

Figure 6 illustrates the experimental setup used in the present experiments. The test column in which water and the gas mixture were brought into mutual contact was made of a transparent poly(methyl methacrylate) (PMMA) pipe (100 mm ID and 1,000 mm long) with its ends closed by a flange-type PMMA top cover and a vertically movable piston-like bottom plate fabricated from PMMA and aluminum, respectively. A glass wire down which water was allowed to flow was fixed on the axis of the column. The upper end of the wire was inserted into a tubular stainless-steel nozzle, which was fixed onto the top cover and connected to an external water reservoir. The lower end of the wire protruded out of the test column through the bottom plate and was inserted into a stainless-steel tube connected to a water-sampling device. The CO_2 and N_2 gases were supplied from high-pressure bombs to a Kofloc PMG-1 gas blender to be mixed at a prescribed proportion and were then allowed to flow into the test column through four ports on the bottom plate. The gas mixture flowed upward in the column at a superficial velocity ~ 29 mm/s and flowed out of the column through four ports on the top cover.

Deionized and distilled water was supplied to the nozzle at a constant flow rate, fell down along the wire to the bottom plate, and flowed into the stainless-steel tube connected to a three-way valve, with which we could make, when necessary, a prescribed volume of water flow into an airtight sampling vial. The water inlet on the bottom plate and the tubing to the sampling device were so designed and operated that, except for a part of a small cavity close to the inlet, they were always filled with liquid water. This was to minimize extra absorption of CO_2 due to gas–water contact outside the *test section*, that is, the space in the test column bordered by the level of the nozzle outlet and the upper surface of the bottom plate. The water sample thus stored in the vial was analyzed later by use of a TOC-500 total organic carbon analyzer (Shimadzu Company, Kyoto) to determine the concentration of CO_2 in it. The concentration thus determined was considered to represent the value of c_L at fall distance x measured from the nozzle outlet to the upper surface of the bottom plate. In each experimental run, water-sampling operations were done successively, changing the elevation of the bottom plate such that x varied from 50 mm to 450 mm at intervals of 100 mm, to obtain a set of $c_L(x)$ data. Such data sets were collected by carrying out 12 runs under 6 different combinations of the 3 operational parameters—d_w, d_n, and $\dot{V}_L$. A few runs were performed under each of some combinations to check the repeatability of the experiments. Also performed were a few additional runs in which no wire was used, so that water drops were released from a nozzle to fall freely in the gas phase until they were collected at the bottom of the test column to be sampled in the same way as in the standard experiments with wires. The $c_L(x)$ data obtained with such free-fall water drops will be compared with those for string-of-beads flow to characterize it as a means of gas absorption.

Results and discussion

The parameter we use below as an index for the effectiveness of the gas-to-liquid CO_2 transfer is the transfer efficiency $E(x)$ defined as follows:

$$E(x) = \frac{c_L(x) - c_{L0}}{c_s - c_{L0}}. \tag{12}$$

The experimental results are plotted, as shown in Figure 7, in the form of $1-E$ against x on a semilogarithmic plane for convenience of interpretation. The $1-E$ vs. x relation for each experimental run must be linear on a semilogarithmic plane, under the conditions that the liquid flow is fully developed and that the overall mass-transfer coefficient is axially uniform. The experimental results shown in Figure 7 indicate that the preceding conditions were approximately satisfied over the major portion of the wire length. The intercept recognized by extrapolating each $1-E$ vs. x relation to $x=0$, the nozzle outlet, is ascribable to an end effect presumably due to relatively strong circulatory flows remaining inside the

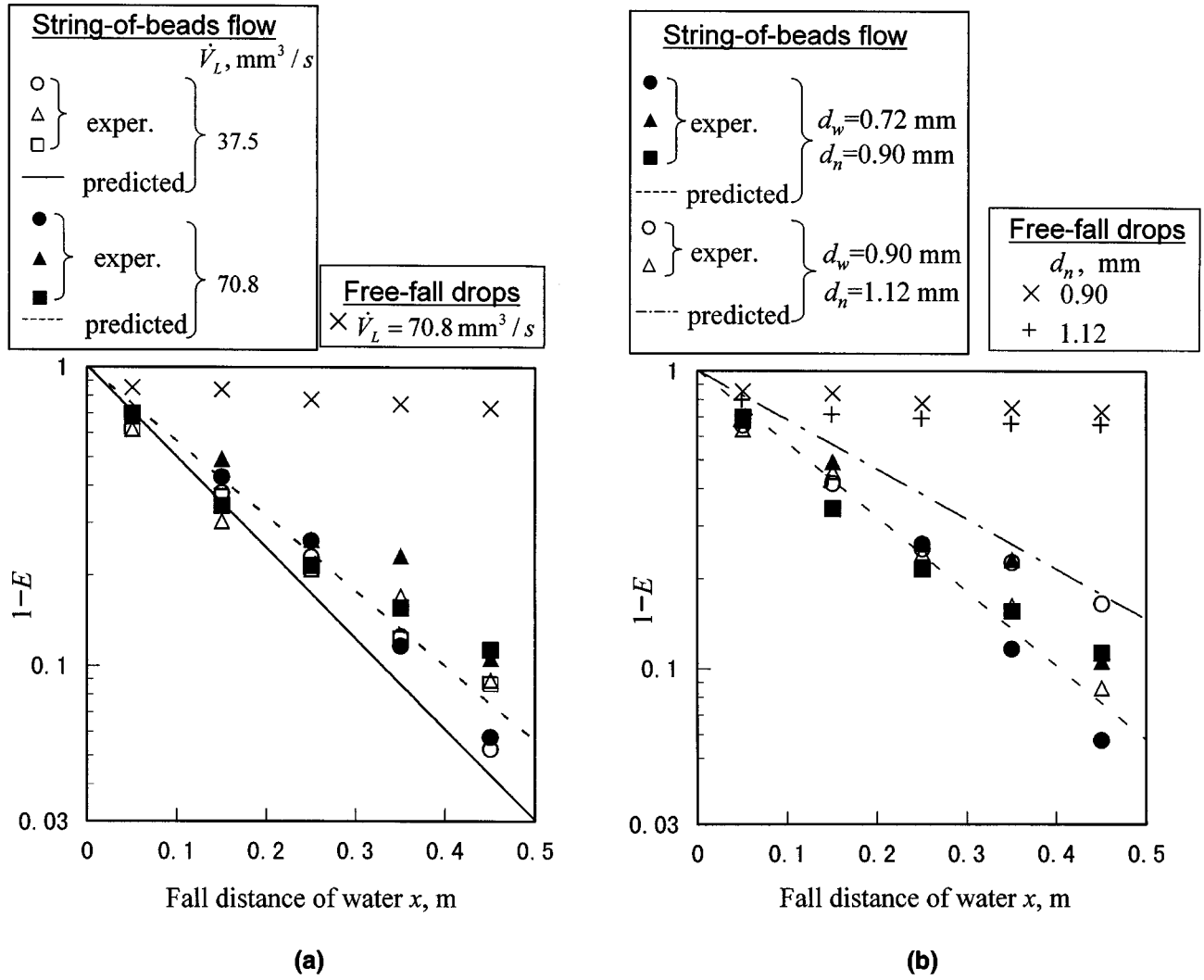

Figure 7. Complementary CO_2-transfer efficiency plotted against fall distance of water.

Compared are the experimental results for isolated drops in free fall, those for string-of-beads flow on wires, and predictions based on the model of string-of-beads flow. (a) Results obtained at two different water flow rates with the same nozzle–wire assembly: $d_w = 0.72$ mm and $d_n = 0.90$ mm. The data for free-fall drops were obtained with the nozzle of $d_n = 0.90$ mm in the absence of any wire. (b) Results obtained with two different nozzle–wire assemblies when the water flow rate was fixed at $\dot{V}_L = 70.8$ mm^3/s. The data for free-fall drops were obtained with two different nozzles ($d_n = 0.90$ mm and 1.12 mm, respectively) used alternatively in the absence of any wire.

beads just after their formation. Also plotted in Figure 7 are the predictions based on the model described in the preceding section of this article and the experimental results for freely falling drops. Note that the higher flow rate of water, $\dot{V}_L = 70.8$ mm^3/s, indicated in Figure 7 corresponds to the critical flow rate, $\dot{V}_{L,\mathrm{cr}}$, beyond which l_d levels off and at which U_d has a minimum, for both of the two nozzle–wire assemblies with which the results for the string-of-beads flows given in Figure 7 were obtained.

The experimental results for the string-of-beads flow plotted in the two diagrams in Figure 7 indicate rather weak dependencies of $E(x)$ on the flow rate of water (Figure 7a) and on the nozzle–wire assembly (Figure 7b). It can be said that only slightly higher $E(x)$ values are available with the lower flow rate, $\dot{V}_L = 37.5$ mm^3/s, and with the finer nozzle–wire assembly, $d_w = 0.72$ mm and $d_n = 0.90$ mm.

The agreement between the predictions due to the model and relevant experimental data is reasonably good despite the highly simplified nature of the model. The predicted, slightly sharper ln $(1-E)$ vs. x slopes can be ascribed to the fact that the model idealizes both the circulations inside individual beads and the film–bead mass exchange.

Also recognized in Figure 7 is a great superiority of the string-of-beads flow on wires over the free fall of discrete drops, which simulates the gas–liquid contact mode in spray columns, on the condition that a particular species to be removed from the gas phase is desirably concentrated in a limited amount of a liquid absorbent.

Vertical-Wire Columns vs. Conventional Gas–Liquid Contactors: Comparative Study

This section aims to show a quantitative comparison of the gas-absorption performance of an imaginary *vertical-wire column* utilizing the string-of-beads flow on multiple wires (see Figure 8) to those of conventional wetted-wall and packed-bed

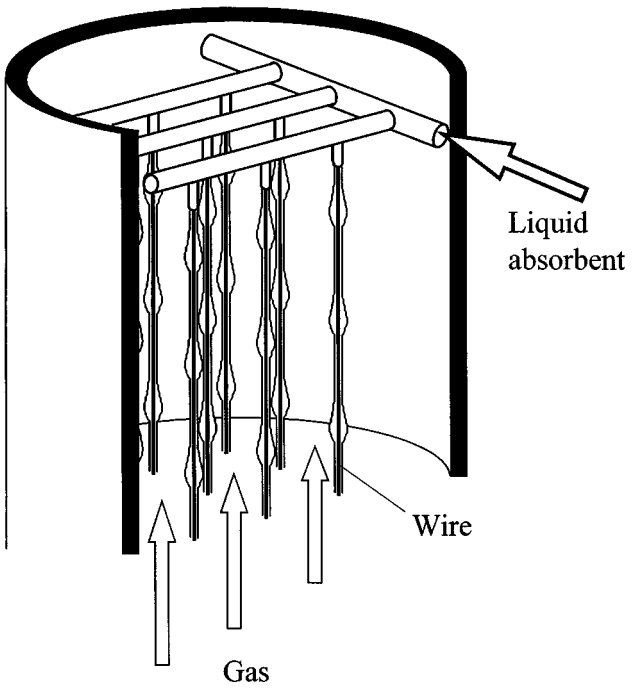

Figure 8. Concept of liquid-inlet portion in a vertical-wire gas–liquid contactor equipped with multiple wires on each of which a string-of-beads flow of liquid absorbent is to be formed.

columns. These columns are assumed to be applied to a common test process that is consistent with the experiments described in the preceding section, that is, the CO_2 absorption by liquid water at a temperature of 20°C under the standard atmospheric pressure, 101.3 kPa. The mass-transfer resistance in the gas phase is assumed to be negligible in every column, compared to that in the liquid-water phase. The water flow rate evaluated in terms of the superficial velocity u_L, that is, the volume flow rate of water divided by the cross-sectional area of each column, is fixed in common with all of the columns; it is rather low relative to the gas flow rate so that the equilibrium CO_2-in-water concentration c_s can be assumed to be constant along the column axis. The performance of each column is evaluated in the form of $1-E$ plotted against x. As for the vertical-wire column, the experimental results shown in Figure 7 can be used as they are. For the wetted-wall and packed-bed columns, we rely on existing empirical correlations for the mass transfer in liquid phases in those types of columns, to estimate $1-E$ vs. x relations. The procedure for such an estimation is outlined below.

The differential mass balance for the species transferred into the liquid film in a wetted-wall column is written as

$$\pi R^2 u_L \frac{dc_L}{dt} = 2\pi(R-\delta_f)\beta_L(c_s - c_L), \qquad (13)$$

where R is the inside radius of the column, x is the vertical distance traveled by the liquid in contact with the gas phase, δ_f is the thickness of the liquid film, and β_L is the coefficient for surface-to-bulk mass transfer in the liquid film. Integration of the preceding equation leads to

$$1-E = \exp\left[-\frac{2(R-\delta_f)\beta_L x}{R^2 u_L}\right]. \qquad (14)$$

Combining Eq. 14 with existing correlations for δ_f (Brotz, 1954) and for β_L (Yih and Chen, 1982), we can calculate $1-E$ as a function of x for each operational condition specified by R and u_L.

The differential mass-balance equation for a packed-bed column can be written, neglecting the column-wall effect, as

$$u_L \frac{dc_L}{dt} = a_{lg}\beta_L(c_s - c_L), \qquad (15)$$

where a_{lg} is the effective liquid–gas interfacial area per unit volume in the packed bed, and β_L is the coefficient for surface-to-bulk mass transfer in the liquid film flowing over the packings. Equation 15 is integrated to give

$$1-E = \exp\left(-\frac{a_{lg}\beta_L x}{u_L}\right). \qquad (16)$$

If we specify the packings and u_L, we can use the empirical correlations due to Onda et al. (1967, 1968) to estimate a_{lg} and β_L, and then use Eq. 16 to calculate $1-E$ as a function of x. In the present calculations, we assumed the use as the packings of quarter-inch Raschig rings, the surfaces of which are characterized by a critical surface tension of 61 mN/m.

Figure 9 compares the $1-E$ vs. x relations for the vertical-wire, wetted-wall, and packed-bed columns while oper-

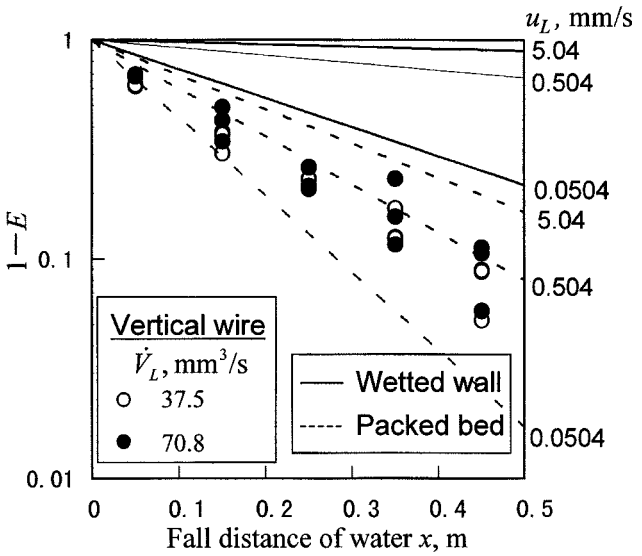

Figure 9. Complementary CO_2-transfer efficiencies vs. fall distance of water in vertical-wire, wetted-wall, and packed-bed columns.

The efficiency–distance relations for the vertical-wire column is represented by the experimental data obtained with the string-of-beads flows on a single wire ($d_w = 0.72$ mm, $d_n = 0.90$ mm). The relations for the wetted-wall and packed-bed columns are due to existing empirical correlations for the liquid-phase-side mass-transfer coefficients in such conventional types of gas–liquid contactors.

ated for CO_2 absorption by liquid water used as the absorbent. The performance of the wetted-wall column is dependent on its size; in Figure 9 its inside diameter is assumed to be 1 m ($R = 0.5$ m). As for the vertical-wire column, the experimental results obtained with the single-wire apparatus (Figure 6) are plotted as they are, assuming no wire-to-wire interaction effect on the CO_2 absorption. Note that N_w, the number of wires to be installed in the column, and ζ_L, the maximum areal fraction of column cross section that could be occupied by the liquid, are simply given by

$$N_w = \pi R^2 u_L / \dot{V}_L \tag{17}$$

and

$$\zeta_L = N_w \left(\frac{d_{d2}}{2R} \right)^2 = \frac{1}{4} \frac{\pi d_{d2}^2 u_L}{\dot{V}_L}, \tag{18}$$

respectively. For the conditions assumed in Figure 9, ζ_L is calculated to be 0.001–0.34; this indicates that the preceding assumption is reasonable, at least for moderate liquid flow rates, $u_L \lesssim 1$ mm/s, at which $\zeta_L \lesssim 0.07$. Figure 9 clearly shows that the vertical-wire column is much superior in the performance of gas absorption to the wetted-wall column of the same size. The vertical-wire column nearly compares with the packed-bed column in absorption performance. This fact suggests that the former is potentially superior to the latter, because the pressure losses imposed on the gas and liquid-water flows are presumably much lower in the former than in the latter.

On the other hand, we should not overlook some technical difficulty accompanying the vertical-wire column design. The number of wires required, N_w, is sometimes large; it varies from 5.6×10^2 (when $u_L = 0.0504$ mm/s and $\dot{V}_L = 70.8$ mm^3/s) to 1.06×10^6 (when $u_L = 5.04$ mm/s and $\dot{V}_L = 37.5$ mm^3/s) under the conditions assumed in Figure 9. How to bundle the wires and how to supply the liquid onto them are the problems that must be solved before the idea of vertical-wire columns can be put into practice. A manifold-type liquid-distributor (Figure 8) may be feasible for N_w for several hundred. For a larger number of wires, a completely different water-distribution scheme should probably be contrived.

Conclusions

This article has presented experimental and analytical examinations of the mechanistic and gas-absorption performance of the string-of-beads flow of liquid water or an aqueous MEA solution on vertical wires. An important finding about the flow itself is that it is not uniquely determined by defining the wire diameter and the liquid flow rate plus the substance of the liquid and the thermodynamic conditions. Rather, the flow is dependent on the condition of liquid release from the nozzle onto the wire. Particular patterns are found in the dependencies of the axial interval, the fall velocity, and the size of the beads on the liquid flow rate.

The experiments of CO_2 absorption by water in the string-of-beads flow have shown that a transfer efficiency as high as 0.9 is obtained with only some 0.5-m fall of water on wires. This result leads to the conclusion that vertical-wire columns utilizing the string-of-beads flow of liquid absorbents can have a considerable advantage over conventional gas–liquid contactors, such as spray columns, wetted-wall columns, and packed-bed columns, in obtaining high transfer efficiencies at the cost of minimal pressure losses imposed on both gas and liquid flows.

A simple analytic model of gas absorption by a nonreacting liquid absorbent in string-of-beads flow has been developed. With the aid of some experimental knowledge of the string-of-beads flow of a given absorbent, the model enables us to predict the performance of the gas absorption. For CO_2 absorption by water, the agreement between the predictions thus obtained and relevant experimental results were found to be satisfactory. This fact indicates the potential utility of the model for saving a great deal of experimental work in designing practical gas-absorption operations that incorporate string-of-beads flows of liquid absorbents.

Acknowledgments

This study was supported in part by a Research Grant from the Iwatani Naoji Foundation. Our thanks are due to M. Ibi and N. Fumino, former students in the Department of Mechanical Engineering, Keio University, for their assistance at the early stages of the study, to Prof. S. Matsumura, Department of Applied Chemistry, Keio University, for his kind instruction in the use of the TOC in his laboratory, and to H. Migita, a student in the Department of Mechanical Engineering, Keio University, for his help in preparing some of the drawings used in this article.

Notation

c_L = time-averaged, mixed-mean value of c at arbitrary axial location
Sh = Sherwood number
t = time
V_d = bead volume

Subscript

d = bead
0 = initial condition before the onset of liquid–gas contact

Literature Cited

Brotz, W., "Über die Vorausberechnung der Absorptionsgeschwindigkeit von Gasen in strömenden Flüssigkeitsschichten," *Chem.-Ing.-Tech.*, **26**, 470 (1954).

Hattori, K., M. Ishikawa, and Y. H. Mori, "Strings of Liquid Beads for Gas–Liquid Contact Operations," *AIChE J.*, **40**, 1983 (1994).

Nozaki, T., N. Kaji, and Y. H. Mori, "Heat Transfer to a Liquid Flowing Down Vertical Wires Hanging in a Hot Gas Stream: An Experimental Study of a New Means of Thermal Energy Recovery," *Proc. 11th Int. Heat Transfer Conf.*, Korean Soc. Mech. Eng., Seoul, Korea, Vol. 6, p. 63 (1998).

Onda, K., H. Takeuchi, and Y. Koyama, "Effect of Packing Materials on the Wetted Surface Area (in Japanese)," *Kagaku Kogaku*, **31**, 126 (1967).

Onda, K., H. Takeuchi, and Y. Okumoto, "Mass Transfer Coefficients Between Gas and Liquid Phases in Packed Columns," *J. Chem. Eng. Jpn.*, **1**, 56 (1968).

Yih, S.-M., and K.-Y. Chen, "Gas Absorption into Wavy and Turbulent Falling Liquid Films in a Wetted-Wall Column," *Chem. Eng. Commun.*, **17**, 123 (1982).

Manuscript received Apr. 30, 1999, and revision received Nov. 1, 1999.